

Accounts of Materials & Surface Research

First-principles Electronic Structure Calculation for Catalyst Design

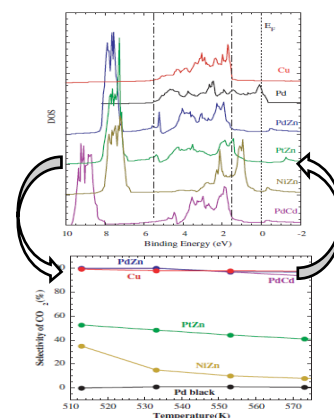
K. Nozawa^a and Y. Ishii^{b*}

^aDepartment of Physics and Astronomy, Kagoshima University, Korimoto, Kagoshima 890-0065, Japan

^bDepartment of Physics, Chuo University, Kasuga, Tokyo 112-8551, Japan

ishii@phys.chuo-u.ac.jp

Alloying of elements is one of the most primitive ways of modifying chemical and physical properties of matter and has been used for improving the properties of metallic elements. Recently, catalysis studied in terms of metallurgy is of increasing interest and represents a rising stream of publications in the community. We review our published works on catalytic functions exhibited by intermetallic compounds and alloys with a special focus on theoretical calculation of the electronic structures. We show that the theoretical calculation can be a promising tool to provide useful information for catalyst design. We present here two examples; one is PdZn intermetallic compound, which exhibits a similar catalytic property to Cu, and the other one is CuNi solid solution, which exhibits a similarity to Pd. We stress the strong correlation between the catalytic activity and the valence electronic structures as a key concept for predicting new candidate materials for catalyst.



Keyword: intermetallic compound, random alloy, first-principles calculation, electronic structure, catalyst design

Kazuki Nozawa received his Ph.D. from Himeji Institute of Technology in 2002 under the supervision of Professor Nobuyuki Shima and Professor Kenji Makoshi. He worked as a postdoctoral researcher and Assistant Professor with Professor Yasushi Ishii at Chuo Univ., then he is currently an Associate Professor in the Department of Physics and Astronomy at Kagoshima Univ. His current research interest includes the correlation between catalytic properties and electronic structures of intermetallic compounds, and also growth mechanisms of single-element quasicrystalline films.



Yasushi Ishii received his PhD from Univ. of Tokyo in 1984 and is currently a Professor of physics in Chuo Univ. His main research is focused on theoretical studies of electronic structures and properties of solids, in particular intermetallic compounds. He is also interested in dynamical aspects of quasicrystals.



First-principles Electronic Structure Calculation for Catalyst Design

K. Nozawa^a and Y. Ishii^b

^aDepartment of Physics and Astronomy, Kagoshima University, Korimoto, Kagoshima 890-0065, Japan

^bDepartment of Physics, Chuo University, Kasuga, Tokyo 112-8551, Japan

1. Introduction

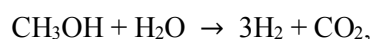
Alloying of elements is one of the most primitive ways of modifying chemical and physical properties of matter and has been used for improving the properties of metallic elements. Depending on combination of elements, material forms either solid solution or intermetallic compound. In particular, intermetallic compound, which possess a completely different structure from that of pure materials with a specific ordered configuration, usually exhibits very different electronic properties from mother elements. Changes in the electronic properties are sometimes very drastic and, in some intermetallic compounds made of metallic elements, covalent rather than metallic nature in the electronic states is suggested.¹⁾ In solid solution, or so-called random alloy, on the other hand, elements are mixed randomly without appreciable macro- or meso-scale segregation. In this case we expect materials exhibiting characteristic properties of both mother elements, but furthermore mixing of elements in nano-scale may cause other effects on microscopic phenomena such as reaction of chemical species.

Recently, catalysis studied in terms of metallurgy is of increasing interest and represents a rising stream of publications in the community.²⁾ Several new forms of catalysts have been developed, and some new insights have been derived within this framework. One of the unique concepts here is “pseudoelement”,

which means that the intermetallic compound shows similar electronic structure and catalytic selectivity to another single element.^{2, 3)} In this account, we review our published works³⁻⁵⁾ with a special focus on theoretical calculation of the electronic structures of intermetallics and alloys and try to show how an intermetallic and alloy can be viewed as a pseudoelement in terms of electronic structure and catalytic selectivity. In section 2, we discuss on PdZn, which is an intermetallic compound with an ordered structure.^{3, 4)} In section 3, we discuss on CuNi, which is a random alloy, where Cu and Ni are distributed randomly on a face-centered cubic lattice.⁵⁾

2. PdZn Intermetallic Compound

Iwasa *et al.*⁶⁾ first discovered that when Pd was supported on ZnO, the catalytic function of Pd was greatly modified, resulting in a highly active and selective catalyst for the steam reforming of methanol (SRM),



a chemical reaction for producing hydrogen. Under SRM, the Pd/ZnO catalyst exhibits a high selectivity of CO₂, comparable with that of Cu-based catalysts. Pd/ZnO is not only highly active for SRM, but also active for the dehydrogenation of methanol to HCOOCH₃⁷⁾, which is normally catalyzed using Cu-based catalysts. The high performance of these reactions has been demonstrated to be due to the

formation of an intermetallic compound, PdZn. It is striking that PdZn compound is catalytically similar to Cu, *i.e.*, an intermetallic compound can replace a metallic element without changing the catalytic function.

PdZn compound forms the $L1_0$ ordered structure, which consists of alternating Pd and Zn layers along (001) axis on a face-centered cubic (fcc) lattice with tetragonal distortion. According to precise x-ray diffraction analysis, lattice parameters for PdZn and isostructural NiZn and PtZn are given as $a=0.290$ nm and $c=0.336$ nm for PdZn, $a=0.274$ nm and $c=0.324$ nm for NiZn, and $a=0.288$ nm and $c=0.353$ nm for PtZn for a body-centered tetragonal (bct) unit cell.⁴⁾ The bct lattice is also described as a face-centered tetragonal (fct) lattice (Fig. 1). Although the fct lattice is not optimal choice of a unit cell, the fct description easily matches the $L1_0$ structure. The structures of pure Cu, Pd, Ni, and Pt are fcc, and the fct description is convenient for direct comparison with the fcc structure. We use the fct description for the Miller indices of the surfaces.

First-principles electronic structure calculations were performed by using the tight-binding linear muffin-tin orbital

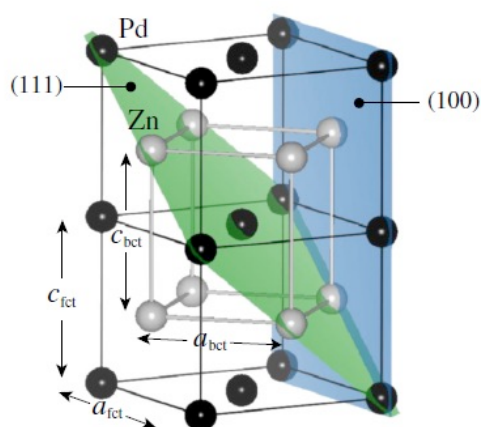


Figure 1. Body-centered tetragonal (bct) and face-centered tetragonal (fct) unit cells of the $L1_0$ structure.

(TB-LMTO) method in the atomic-sphere approximation (ASA).⁸⁾ Electron–electron interaction is taken into account within the local-density approximation in the density functional theory.⁹⁾ Although the lattice constants and atomic positions for slab calculations are relaxed using a plane-wave basis code^{10,11)} with projector-augmented wave potentials,¹²⁾ no significant surface relaxation is obtained.

Calculated electron densities of states (DOSs) for pure Cu and PdZn are shown in Fig. 2. In order to understand the alloying effects, the calculated DOS for pure Pd is also shown for comparison. A broad sp band extends up to the Fermi level (E_F) and at approximately 2 eV below E_F , a pronounced peak due to filled $3d$ electron states is observed for pure Cu. Similar features coming from different origins, a broad sp state crossing E_F and a peak due to filled $4d$ electron states of Pd at approximately 2 eV below E_F , are observed in the DOS for PdZn. We note that the $4d$ states of pure Pd are located at E_F while the Zn spectrum consists of a $3d$ band centered at 8 eV below E_F and a broad sp band

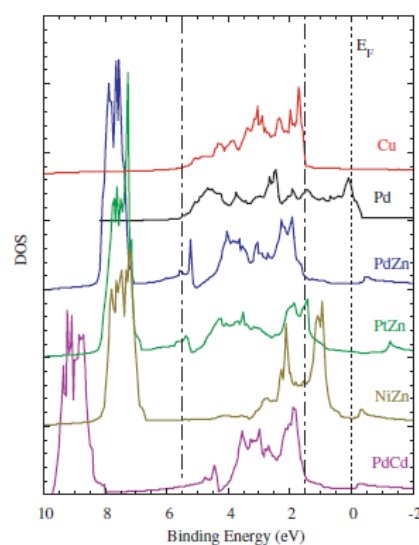
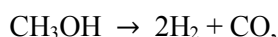


Figure 2. The DOSs for fcc Cu and Pd, and PdZn, PtZn, NiZn and PdCd of the $L1_0$ type.

overlapping the d band. Thus, the most remarkable change due to the formation of the compound is an apparent suppression of the Pd $4d$ states near E_F .

To demonstrate that the catalytic properties correlate with the valence electronic structures, the catalytic selectivity in the SRM was tested for PdZn, NiZn, PtZn, pure Cu and pure Pd. It is known that the SRM is catalyzed using Cu-based catalysts whereas Pd shows a high activity in the decomposition of methanol (DM),



which produces CO rather than CO_2 . It is found that the selectivity of CO_2 for both pure Cu and PdZn is almost 100% at the reaction temperature 510-570 K, but that for pure Pd is almost 0%. As is seen in Fig.2, the distance of the d -band top from E_F is in the order of PdZn > PtZn > NiZn. It turns out that this order corresponds well to the order of CO_2 selectivity. From these observations, we speculate that a similarity in catalytic selectivity for PdZn and pure Cu is due to their similar valence electron DOSs. In other words, intermetallic PdZn behaves like Cu for the SRM because of similarity in the valence electronic DOS and thus PdZn can be regarded as a *pseudoelement* of Cu. To test the idea of the strong correlation between the catalytic activity and the valence electronic structures, the catalytic selectivity of isostructural PdCd, which has a similar DOS to PdZn and pure Cu as shown in Fig.2, was studied. It was found that the selectivity of CO_2 for the SRM reaction reaches the same level as those of PdZn and Cu. This suggests possibility of prediction of catalytic functions based on the calculated valence electron DOS.

The electron configurations of isolated Pd and Zn atoms are $d^{10}s^0$ and $d^{10}s^2$, respectively. If one expects naively that an *average* electron

configuration $d^{10}s^1$ is realized in PdZn compound, similarity in the electronic DOSs of PdZn and Cu seems reasonable. However, mechanism of modification of the electronic structure in PdZn is not simple and beyond a rigid-band picture. To understand mechanism of the Pd $4d$ states suppression near E_F in PdZn by alloying, we show the band dispersion for some hypothetical structures. In Fig. 3, we show the band dispersions of (a) fcc Pd ($a=0.389$ nm) and (b) hypothetical PdZn where the lattice constants a and c are taken as 0.378 nm to realize ordering on the fcc lattice. The curve width indicates the amount of the d_{yz} and d_{zx} components extending in the nearest-neighbor directions. One can see that the bonding–antibonding splitting of the d_{yz} and d_{zx} bands vanishes in PdZn at the Γ and M points. The d_{yz} and d_{zx} states extend in the nearest

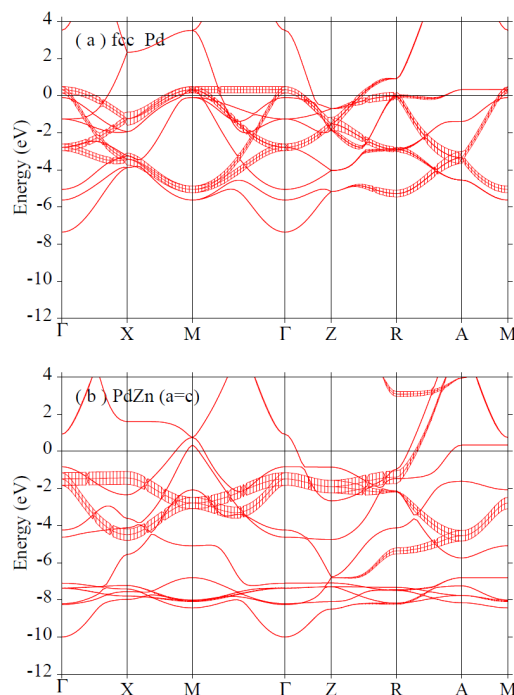


Figure 3. The band dispersions of (a) fcc Pd ($a=0.389$ nm) and (b) hypothetical PdZn with $a=c=0.378$ nm. The d_{yz} and d_{zx} components are indicated by the curve width.

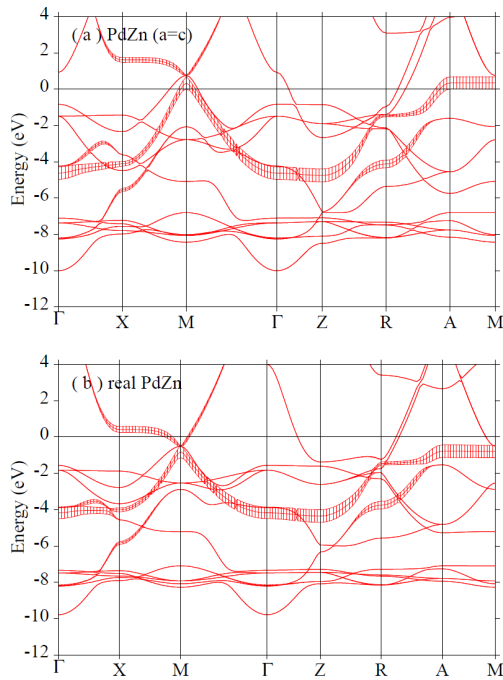


Figure 4. The band dispersions of (a) hypothetical PdZn with $a=c=0.378$ nm and (b) real PdZn with $a=0.411$ and $c=0.336$ nm. The $d_{x^2-y^2}$ components are indicated by the curve width.

neighbor Pd–Zn directions. Since the Zn-3d band is located at several eV below the Pd-4d band, the d - d mixing between Zn and Pd is considerably small compared with that between Pd. Thus, the d_{yz} and d_{zx} bands at approximately -2 eV are in nonbonding nature in PdZn.

The reduction in the bandwidth is also due to the tetragonal lattice distortion in PdZn. In comparison with the hypothetical PdZn ordered structure on the fcc lattice, the real PdZn compound showed c/a ratio reduced by 20%. This leads to reduction in the degree of band dispersion in the ab -plane. In Fig. 4, the band dispersions for (a) hypothetical PdZn with $a=c=0.378$ nm and (b) real PdZn with $a=0.411$ and $c=0.336$ nm are compared, where the amount of the $d_{x^2-y^2}$ components are indicated by the curve width. The splitting of the dispersionless $d_{x^2-y^2}$ branches on the Γ -Z and A-M lines is

determined by hopping in the ab -plane and reduced in the real PdZn.

The catalytic reaction proceeds on solid surfaces and the catalytic selectivity is usually sensitive to the surface state. Since our arguments so far are based on the bulk electronic structure, we should check the surface effects more precisely. To do this, the electronic DOS at surfaces were calculated with a slab model. For the (001) and (100) surfaces, a $1 \times 1 \times 12$ supercell was adopted where a single tetragonal unit cell consists of two atomic layers. In the present calculations, 11 atomic layers were replaced with empty sites to represent vacuum layers. For the (111) surface, a similar 24-atomic-layer model was adopted where 11 layers are replaced with empty sites. In the (001) case, either Pd or Zn appears alternatively in a single atomic layer, whereas both elements appear in a single atomic layer

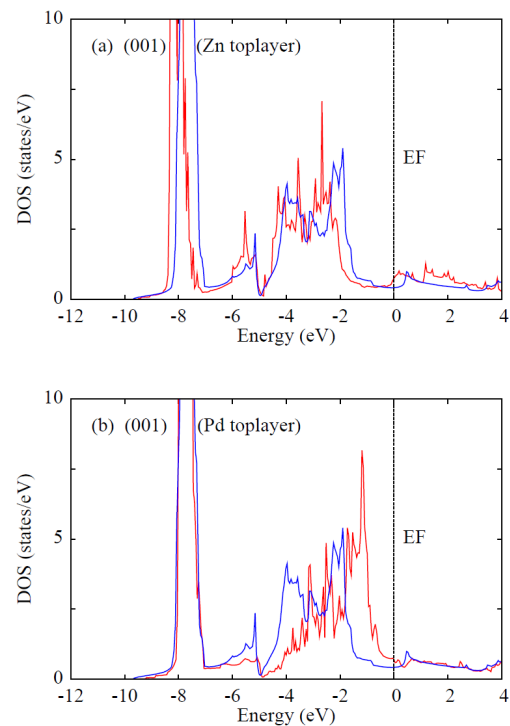


Figure 5. The surface DOS for (a) (001)Zn and (b) (001)Pd slabs (red). The bulk DOS is shown for comparison (blue).

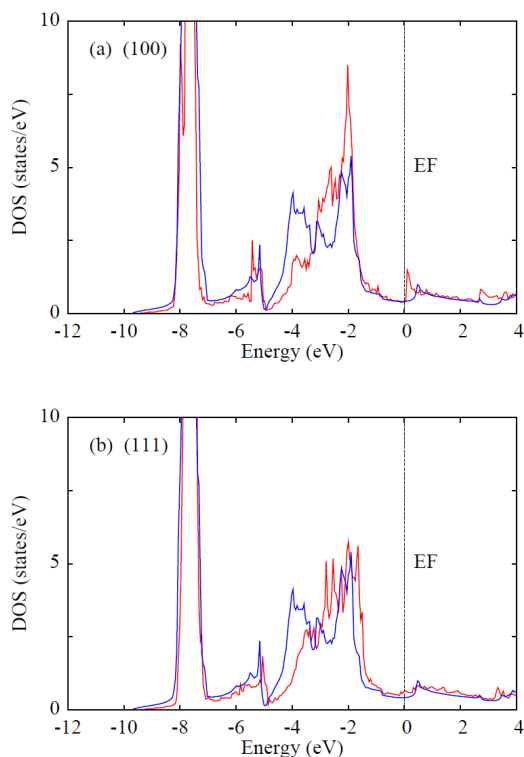


Figure 6. The surface DOS for (a) (100) and (b) (111) slabs (red). The bulk DOS is shown for comparison (blue).

with a bulk composition for the (100) and (111) surfaces. In Fig. 1, the (100) and (111) planes are shown. The x - and y -axes are parallel to the lattice vectors for the fct lattice, and so the d_{xy} orbital has a tail in the direction of the nearest-neighboring atom in the ab -plane.

Figure 5 shows the local DOSs for the Pd and Zn topmost layers of the (001) surfaces together with the bulk DOSs for PdZn. The narrow band at -8 eV is the semi-core Zn-3d band, but we focus first on the Pd-4d valence band above -6 eV. Although the (001) plane is less stable and is not expected to appear on the surface, we show how the composition at surface affects the valence electronic DOS. Figure 5(a) shows the case where Zn atoms appear at the topmost of the (001) surface, to which we will refer as the (001)Zn case hereafter. One can see that the d -bands shift to higher binding energies

compared with the d band of bulk layers. In contrast, Fig. 5(b) shows the case where Pd atoms appear at the topmost of the (001) surface [(001)Pd case]. The d band shifts to lower binding energies, *i.e.*, the top of the d band toward the Fermi level. To evaluate the electronic potentials near surface within the ASA, the effective potential at the atomic sphere surface is used. Technical detail is given in the original article.¹⁴⁾ It is found that the potential at the topmost Pd sites for the (001)Pd slab is shallower by 1.6 eV and that at the second topmost Pd sites for the (001)Zn slab is deeper by 1.0 eV than that for the bulk. This difference is consistent with the shifts of the Pd-4d band near the surface.

A few remarks on the remarkable shift of the Zn-3d band for the (001)Zn slab should be given. Surface termination makes electrons spread out to the vacuum from the surface layer. This makes the topmost surface layer positively charged, hence the deeper core potential. Since the Zn-3d state is more localized in the core region, the semi-core band shifts to the larger binding energies. For the Zn sites on the second topmost layer in the (001)Pd slab and the valence states like the Pd-4d band, the level shift caused by the deep core potential is less remarkable.

Figure 6 shows the calculated valence electronic DOSs at the (100) and (111) surfaces for PdZn. The surface DOSs in the both cases are those for the topmost layer. The Pd-4d band top in the surface DOS for the (100) surface remains at almost the same position as that in the corresponding bulk case. The d -band top for the (111) surface is also almost the same as that of the bulk, but shows a slight shift (by 0.1 eV) toward the Fermi level. The slight shift of the d band in the (111) case is caused by splitting of the degenerate d_{yz} and d_{zx} states due to lower symmetry of the (111) surface.

The most remarkable difference of the surface DOS from the bulk DOS is a missing peak at -4 eV. Detailed orbital analysis of the bulk DOS shows that the peak at -4 eV in the Pd-4*d* band is composed mainly of the d_{xy} and d_{3z^2-1} orbitals, which extend toward the first and second neighboring Pd atoms, respectively. As the neighboring Pd-Pd pairs are broken at the (111) and (100) surfaces, the bonding-antibonding splits of these orbitals is reduced, leading to the narrower *d* band. The peak at -2 eV in the bulk DOS, on the other hand, is a contribution of the d_{yz}/d_{zx} and $d_{x^2-y^2}$ states. As discussed above, the d_{yz}/d_{zx} states are nonbonding because these states extend in the direction of neighboring Zn sites. Therefore, the peak near -2 eV is not significantly changed by the breaking of the Pd-Zn pairs at the surface. In contrast to those in the (100) and (111) cases, the total *d*-bandwidth for the (001) surfaces is similar to that for the bulk. This is partly because neighboring Pd-Pd bonds are not broken by surface termination in the (001) cases.

The relative stability of different surfaces was studied by Chen *et al.* for PdZn and PtZn.¹³⁾ It was found that the surface energies for the (111) and (100) surfaces are much smaller than that for the (001) surface. As noted above, either Pd or Zn appears in a single atomic layer for the (001) surface whereas both elements appear in a single atomic layer with a bulk composition for the (100) and (111) surfaces. Chen *et al.* speculate that strong Pd-Zn bond breaking for the (001) surface is responsible for the higher surface energy. According to the analysis of the band dispersion, however, a nonbonding nature for Pd-Zn bonds is suggested in the intermetallic PdZn. Charge transfer in solid state is somewhat controversial because the amount of charge

assigned to an atom depends on the choice of volume around it. Friedrich *et al.*¹⁴⁾ estimated the charge transfer in PdZn based on the theory of Atoms in Molecules¹⁵⁾ and concluded that Pd is more electronegative than Zn. For the (001) surface terminated by a layer comprising either electronegative or electropositive elements, additional loss of the electrostatic (Madelung) energy is needed. To understand difference in the surface energies, further analysis of the bonding nature will be helpful.

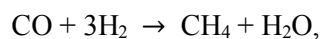
As shown in Fig. 6, the top of the *d*-band for the (100) and (111) surfaces of Pd-Zn is at the nearly same position as the bulk ones. Ganduglia-Pirovano *et al.* studied the potential, core-level and *d*-band shifts for transition-metal surfaces.¹⁶⁾ They argued that, for late-transition metals, the decrease in the *d*-band width caused by the bond-breaking at the surface induces a charge transfer from the *s*- and *p*-states to the *d*-states, which increases the Coulomb repulsion in the *d*-states and shifts the *d*-band center upward to the Fermi level. We expect a similar mechanism for the *d*-band shift in the present intermetallic compound. Namely, the bond-breaking of Pd-Pd pairs at the surface leads to the decrease in the *d*-band width and the shift of the *d*-band center to the Fermi level. The *d*-band narrowing and the shift toward the Fermi level makes the *d*-band top pinned at almost the same position as that in the bulk.

We have investigated the surface DOSs for PdZn of the L1₀-type structure. The slightly shallower potential in the surface layer and bond breaking at the surface lead to the surface *d* band with the top located at nearly the same position as the bulk DOS. So similarity in the catalytic properties of PdZn and Cu can be attributed to similarity in the bulk electronic structures, or more precisely, the position of the

d band. Based on the strong correlation between the catalytic activity and the valence electronic structures, one can propose new candidate materials exhibiting a similar catalytic activity. This suggests that the first-principles electronic structure calculations could provide useful information for catalyst design. In next section, we present another example of the strong correlation between the catalytic activity and the valence electronic structures for random alloy, which does not form intermetallics.

3. CuNi Solid Solution

Cu and Ni are adjacent elements in the periodic table and form a solid solution on a fcc lattice with no ordered phase. The *3d* band for Cu extends from 5-6 to 1-2 eV below E_F as shown in Fig.2 while the top of the *3d* band for Ni is located at E_F with slightly wider band width than Cu (see below). The *3d* band for a CuNi solid solution is then expected to extend over the energy range from 5-6 eV below E_F to just above E_F , which is similar to the *4d* band in Pd. Encouraged by the strong correlation between the catalytic activity and the valence electronic structures demonstrated for PdZn, Tsai *et al.* studied the catalytic activities of a CuNi solid solution and Pd.⁵⁾ The product selectivity for reactions involving methanol and water was again used as a reference for characterizing the catalytic property. Cu is known as the best catalyst for the SRM and Pd shows high activity for the DM. It was confirmed that the CO₂ selectivity is almost 100% for Cu but the CO selectivity is almost 100% for Pd at the reaction temperature above 500K. Pure Ni shows more complicated behavior and it was speculated that Ni catalyzes the DM and



at higher temperatures. For a CuNi solid solution, the CO selectivity as high as Pd was observed. Interestingly, alloyed CuNi shows completely different activities from physical mixture of Cu and Ni catalysts and thus alloying in nano-scale is very essential for realization of the catalytic similarity.

To confirm similarity in the electronic structures in CuNi and Pd, first-principles electronic structure calculations were performed by two different methods. The bulk DOS was calculated by the TB-LMTO method in the ASA.⁸⁾ The electron-electron interactions were accounted for within the local-density approximation in the density functional theory.⁹⁾ For disordered CuNi alloys, we employed a 3×3×3 supercell of a fcc lattice where Cu and Ni are randomly distributed on the lattice points. The atoms are relaxed to their force-free positions using a plane-wave basis code but the displacements of atoms are less than 0.002 nm. As CuNi forms a continuous solid solution and its lattice parameter exhibits a nearly linear relationship, we assume the lattice parameter of the supercell as 1.06 nm. The DOS was calculated using 4×4×4 irreducible *k*-points. Calculations of a slab model were performed using the Vienna ab initio simulation package (VASP)^{10,11)} with the projector-augmented wave method.¹²⁾ Here we show the (111) and (001) cases. The slab model consisted of seven atomic layers and the vacuum layer with the same thickness as the slab. For the (111) slab model, each atomic layer contains 30 randomly distributed Cu and Ni atoms in a single layer and the unit cell of the slab model was orthorhombic with lattice parameters of 12.5, 13.0, and 24.5 Å. For the (001) model, each layer contains 25 atoms with

the orthorhombic cell of $12.5\text{Å}\times 12.5\text{Å}\times 21.2\text{Å}$. The plane-wave cut-off energy was taken to be 300 eV. After all the atoms except those in the central layer had relaxed to their force-free positions with a $3\times 3\times 1$ k -point mesh, the DOS was calculated using a finer mesh of k points.

Figure 7(a) shows the total DOS for random CuNi calculated by the TB-LMTO for a $3\times 3\times 3$ supercell and the local DOSs at Cu and Ni sites. The $3d$ -band extends from 5-6 eV below E_F up to the Fermi level where the lower and higher energy regions are contributions from Cu- $3d$ and Ni- $3d$ states, respectively. In Fig. 7(b), we show the DOSs for pure Pd, Cu and Ni on a fcc lattice with the lattice parameters for the pure metals. For fcc Cu, the $3d$ -band extends from 5-6 to 1-2 eV below E_F whereas it extends from 4-5 eV below E_F to the Fermi energy for fcc Ni. Comparing the local DOSs at Cu and Ni sites in random CuNi with the DOSs for fcc Cu and

Ni, one can see that the total DOS of CuNi appears similar to the superposition of DOS of pure Cu and Ni. This may be a characteristic of random alloys of miscible elements. It should be stressed here that Cu and Ni atoms are mixed in nano-scale in CuNi solid solution and thus chemical species near catalyst could interact with the d states in the range covered by both of the Cu- $3d$ and Ni- $3d$ bands. As demonstrated in Fig.7(b), the energy range covered by the Pd- $4d$ band starts from the 5-6 eV below E_F , which coincides with the bottom of the Cu- $3d$ band, and ends up to E_F , which coincides with the top of the Ni- $3d$ band. This means that the total DOS for CuNi solid solution is located at almost the same position as the $4d$ band in pure Pd. So we expect CuNi shows similar catalytic properties to Pd, rather than those of Cu and Ni.

To evaluate the surface effects, we performed slab calculations for various surfaces. The (111) plane with the highest surface density is considered to be the most stable surface for fcc metals. We show here the results for the (111) surface and the (001) surface as well for comparison. After the relaxation of atomic positions, a tiny buckling, where Cu atoms are more likely to extrude towards the vacuum than Ni (0.07Å for the (111) and 0.1Å for the (001), which correspond to 4-6 % of the interlayer distances), was obtained. As the amount of the buckling is very tiny, we expect no significant surface segregation in real samples.

Figures 8 and 9 show the DOSs for the (111) and (001) slab models, respectively. The results are almost similar and no significant difference between two surfaces is observed. Figures 8(a) and 9(a) show the DOS for the surface layer and decomposition to the local DOS at Cu and

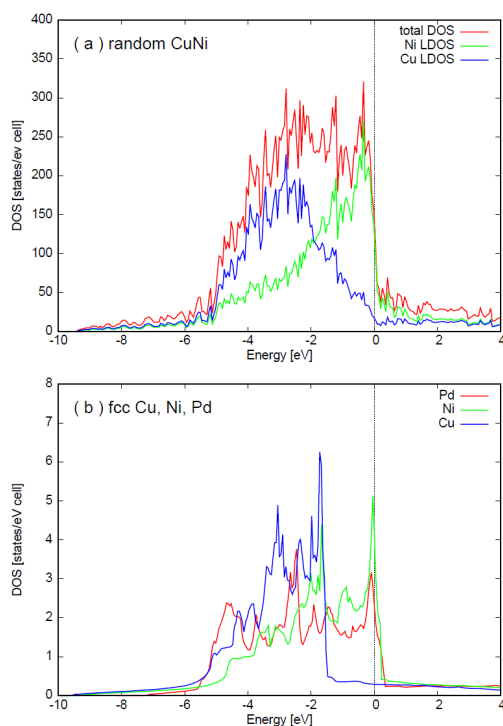


Figure 7. (a) The DOS for random CuNi together with the local DOSs at Cu and Ni sites. (b) the DOSs for fcc Pd, Ni and Cu.

Ni sites. Here we confirm that Ni and Cu are responsible for the higher and the lower energy regions, respectively, in the valence band DOS of CuNi. Figures 8(b) and 9(b) show comparison of the DOS at the surface layer and the bulk one. Those states at 4-5 eV below E_F near the bottom of the d band are depressed and the states just below E_F are enhanced in the surface DOS. These features are usually

observed in the surface DOS for fcc metals and are considered to be due to reduction of the bonding states by surface termination.¹⁷⁾ Figures 8(c) and 9(c) show comparison of the surface DOS for random CuNi and fcc-Pd. Except for the DOS near the d -band bottom depressed for CuNi in comparison with Pd, the band widths for CuNi and fcc-Pd are almost similar. Thus we suppose that the CuNi surface

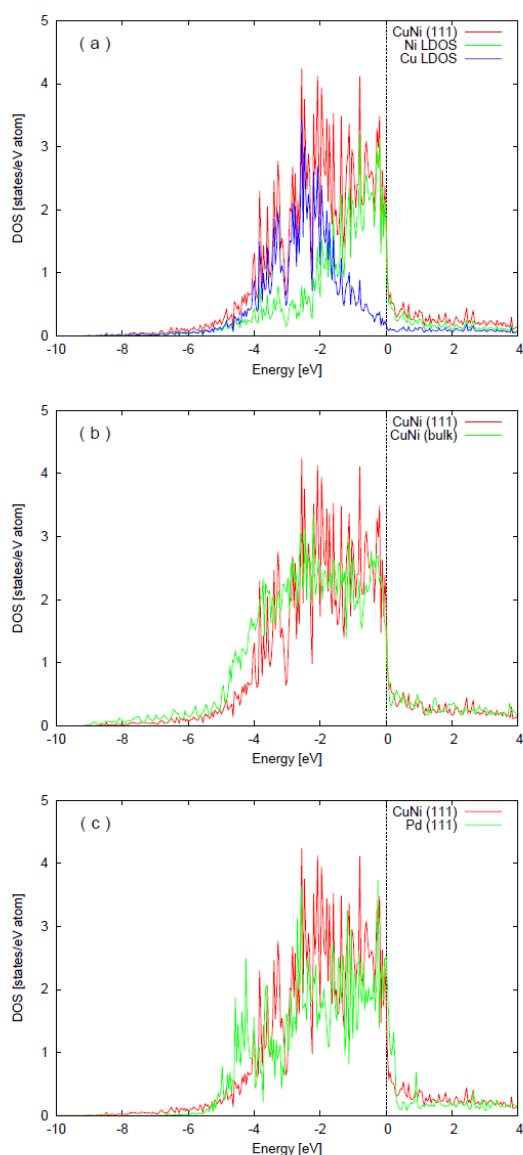


Figure 8. The DOSs for the (111) surface of CuNi (red). Comparisons with (a) the local DOSs at Cu and Ni sites, (b) the bulk DOS and (c) the surface DOS of fcc Pd.

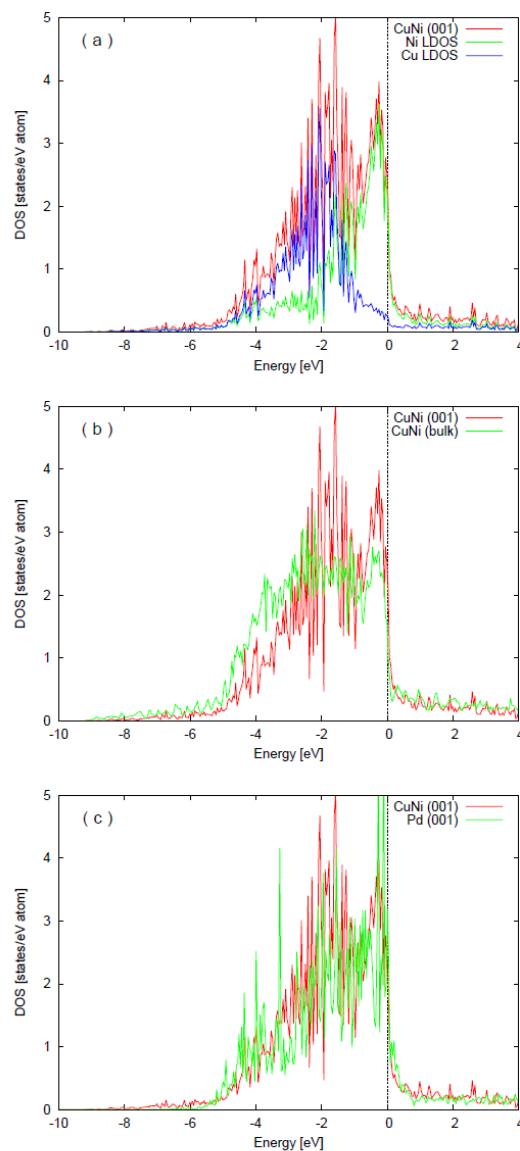


Figure 9. The DOSs for the (001) surface of CuNi (red). Comparisons with (a) the local DOSs at Cu and Ni sites, (b) the bulk DOS and (c) the surface DOS of fcc Pd.

provides the catalytic function very similar to fcc-Pd.

The valence electronic structures in random alloys of miscible elements are not modified so drastically as in intermetallic compounds. The total DOS for random alloys looks like the superposition of the DOSs of pure elements. However, since the elements are mixed in nano-scale, chemical species near the alloy surface can interact with the *d* states extending a wider energy range comprising the *d* states of both elements. This must be the reason why solid solutions work as pseudoelements. Certainly the first-principles calculations will provide useful information for combination of elements with the desirable valence electronic spectrum.

4. Concluding Remarks

We have presented the first-principles calculation of the electronic structures for intermetallics and alloys, which was aimed to give theoretical foundation for the concept of *pseudoelement* supported by the strong correlation between the catalytic activity and the valence electronic structures. It was shown that one can propose new candidate materials exhibiting a similar catalytic activity from the theoretical calculation. We stress that the concept of pseudoelement proposed for intermetallics is also applicable to random alloys where constituent elements are mixed in nano-scale. Nano-scale mixture of elements provides the valence electron spectrum similar to another single element because its valence band extends in a wide range containing the valence spectra of all individual elements. The first-principles calculation can provide information on possible combination of elements.

Computer-aided material design is one of the recent trends in material science and engineering. Here we demonstrated usefulness

and potential of the first-principles calculation in a rather primitive way. More extensive compilation of fundamental data from the first-principles calculation must be desirable for further application of the pseudoelement concept and practical catalyst design.

5. Acknowledgements

Works presented here have been done in collaboration with An-Pang Tsai (Tohoku Univ.), Satoshi Kameoka (Tohoku Univ.), and Masahiko Shimoda (NIMS). We appreciated exciting collaboration and fruitful and stimulating discussions in these studies.

References

- 1) K. Nozawa and Y. Ishii, *Phys. Rev. Lett.* **2010**, 104, 226406.
- 2) A. P. Tsai, S. Kameoka, K. Nozawa, S. Shimoda and Y. Ishii, *Acc. Chem. Res.*, **2017**, 50 2879-2885.
- 3) A. P. Tsai, S. Kameoka, and Y. Ishii, *J. Phys. Soc. Jpn.*, **2004**, 73, 3270.
- 4) K. Nozawa, N. Endo, S. Kameoka, A. P. Tsai, and Y. Ishii, *J. Phys. Soc. Jpn.*, **2011**, 80, 064801.
- 5) A. P. Tsai, T. Kimura, Y. Suzuki, S. Kameoka, M. Shimoda and Y. Ishii, *J. Chem. Phys.*, **2013**, 138, 144701.
- 6) N. Iwasa, S. Masuda, N. Ogawa, and N. Takezawa, *Appl. Catal.*, **1995**, A 125, 145.
- 7) N. Takezawa and N. Iwasa, *Catal. Today*, **1997**, 36, 45.
- 8) O. K. Andersen, O. Jepsen, and D. Glötzel, *Highlight of Condensed Matter Theory*, edited by F. Bassani, F. Fumi, and M. P. Tosi (North-Holland, New York), **1985**, p. 59.
- 9) P. Hohenberg and W. Kohn, *Phys. Rev.*, **1964**, 136, B864; W. Kohn and L. J. Sham, *Phys. Rev.*, **1965**, 140, A1133.
- 10) G. Kresse and J. Hafner, *Phys. Rev. B*, **1993**, 47, 558.

- 11) G. Kresse and J. Furthmüller, *Phys. Rev. B*, **1996**, 54, 11169.
- 12) G. Kresse and D. Jourbert, *Phys. Rev. B*, **1999**, 59, 1758.
- 13) Z.-X. Chen, K. M. Neyman, A. B. Gordienko, and N. Rösch, *Phys. Rev. B*, **2003**, 68, 075417.
- 14) M. Friedrich, A. Ormeci, Y. Gurin and M. Armbrüster, *Z. Anorg. Allg. Chem.* **2010**, 636, 1735.
- 15) R. F. W. Bader, “*Atoms in Molecules: Quantum Theory*”, Oxford Univ. Press, **2003**.
- 16) M. V. Ganduglia-Pirovano, V. Natoli, M. H. Cohen, J. Kudrnovsky and I. Turek, *Phys. Rev. B*, **1996**, 54, 8892.
- 17) J. R. Smith, J. G. Gay and F. J. Arlinghaus, *Phys. Rev. B*, **1980**, 21, 2201.